Earthline Journal of Chemical Sciences
E-ISSN: 2581-9003; CODEN: EJCSB4
Volume 10, Number 1, 2023, Pages 77-91
https://doi.org/10.34198/ejcs.10123.7791

DFT Treatment of Some Cantharidine Isomers and Some Radicals from Them

Lemi Türker

Department of Chemistry, Middle East Technical University, Üniversiteler, Eskişehir Yolu No: 1, 06800 Çankaya/Ankara, Turkey; e-mail: lturker@gmail.com; lturker@metu.edu.tr

Abstract

Cantharidine (cantharidin) has been used as a medicine for centuries for many purposes. It is also known for its anticancer properties. In the present study, some cantharidine isomers and some radicals from them are considered within the realm of density functional theory. The isomers have been subjected to B3LYP/6-311++G(d,p) level of theory and the radicals from them are treated at the level of UB3LYP/6-31+G(d) level. The isomers considered are stereoisomers having the methyl groups at different stereo orientation. The calculations have revealed that the isomers are all thermally favorable and electronically stable. In each case, the mono radical formed from the isomer considered by the homolytic cleavage of C-H bond at the α-position of the etheric oxygen atom. These radicals are also thermally favorable and electronically stable. Various calculated properties of the isomers and the radicals have been harvested and discussed.

1. Introduction

Cantharidine (see Figure 1A) (named as *exo,exo*-2,3-dimethyl-7-oxobicyclo[2.2.1]heptane-2,3-di-carboxylic acid anhydride or exo-1,2-cis-dimethyl-3,6-epoxyhexahydrophthalic anhydride whereas the preferred IUPAC name is 3a*R*,4*S*,7*R*,7a*S*)-3a,7a-Dimethylhexahydro-4,7-epoxy[2]benzofuran-1,3-dione) as a bioactive ingredient, can be isolated from Chinese blister beetles *Mylabris phalerata* or *M. cichorii* and despite its poisonous effects on several organs, historically cantharidine has been used as a medicine for centuries [1,2,3]. Its herbicidal, pesticide, hair growth stimulation and aphrodisiac properties exploited in traditional medicine [4].

Cantharidine is also known for its anticancer properties [4]. However, cantharidine contains in its structure a cyclic anhydride moiety which reacts with nucleophiles present in the biological

Received: February 13, 2023; Accepted: March 17, 2023; Published: March 21, 2023

Keywords and phrases: cantharidine isomers; antitumor; radicals; UV-VIS spectra; density functional.

surrounding and this in turn induces toxicity [4]. Recently, it has been used as a chemical precursor for the development of novel bioinsecticides [5].

Cantharidine and its analogs have all kinds of antitumor activities and their efficacies are also different. Accordingly, their cytotoxicities are of great difference, accompanied by diverse acting mechanisms. The interesting structure-activity relationship not only provides a guide to synthesize new compounds which may have more potent activity and low cytotoxicity, but also offers the mechanisms of cytotoxicity. Overall, cantharidine and its analogs have a future with enormous possibilities for the science and industry of antitumor medicine [6].

Various articles have been published on cantharidine that can treat human hepatoma, pancreatic cancer, colon cancer, oral carcinoma, bladder cancer, breast cancer and human leukemia [7-15], *Condyloma Acuminatum* (a sexually transmitted viral disease caused by the human papilloma virus) [16], treatment of *Molluscum Contagiosum* [17]. Cantharidine is specifically absorbed by lipids in the membrane of epidermal keratinocytes where it activates the release of neutral serine proteases [18].

In the present study, some isomers of cantharidine as well as the radicals formed from them at α-position of the etheric oxygen atom have been considered for a density functional treatment.

2. Method of Calculations

In the present study, all the initial geometry optimizations of the structures leading to energy minima have been achieved by using MM2 method then followed by semi empirical PM3 self-consistent fields molecular orbital (SCF MO) method [19,20] at the restricted level [21]. Afterwards, the structure optimizations have been managed within the framework of Hartree-Fock (HF) and finally by using density functional theory (DFT) at the level of B3LYP/6-311++G(d,p) [22,23]. The radical species are treated at the level of UB3LYP/6-31+G(d) level. It is worth mentioning that the exchange term of B3LYP consists of hybrid Hartree-Fock and local spin density (LSD) exchange functions with Becke's gradient correlation to LSD exchange [24]. Also note that the correlation term of B3LYP consists of the Vosko, Wilk, Nusair (VWN3) local correlation functional [25] and Lee, Yang, Parr (LYP) correlation correction functional [26]. In the present study, the normal mode analysis for each structure yielded no imaginary frequencies for the $3N–6$ vibrational degrees of freedom, where N is the number of atoms in the system. This search has indicated that the structure of each molecule corresponds to at least a local minimum on the potential energy surface. Furthermore, all the bond lengths have been thoroughly searched in order to find out whether any bond cleavage occurred or not during the geometry optimization process. All these computations were performed by using SPARTAN 06 [27].

3. Results and Discussion

Figure 1 shows the side and top views of the optimized structures of the isomers considered

and direction of their dipole moment vectors as well. Structure-A stands for cantharidine. Others differ from cantharidine only by the stereo arrangement of the methyl groups. The anhydride moiety consequently varies its stereo form. In these isomers there exist four stereo centers (see Figure 1).

Figures 2 and 3 show the electrostatic potential (ESP) charges on atoms of the isomers and the ESP maps of the isomers, respectively. Note that the ESP charges are obtained by the program based on a numerical method that generates charges that reproduce the electrostatic potential field from the entire wavefunction [27]. As seen in the figure stereochemistry highly affects the ESP charges even on the anhydride oxygen atom. Note that in their optimized geometries all the isomers considered possess C1 symmetry. Therefore, atoms occupying symmetrical positions in the structural formulas are different, hence the charges (consequently the dipole moment vectors both numerically and directionally) and some other properties of the isomers considered have been affected by stereo chemical variations (see Table 1).

The magnitude of dipole moments and the polarizability values follow the order of A>C>B and A>B>C, respectively. As seen in the table structure-A (cantharidine) is solvated better than the other isomers considered. The solvation order arises from the intricate function of various factors listed in Table 1.

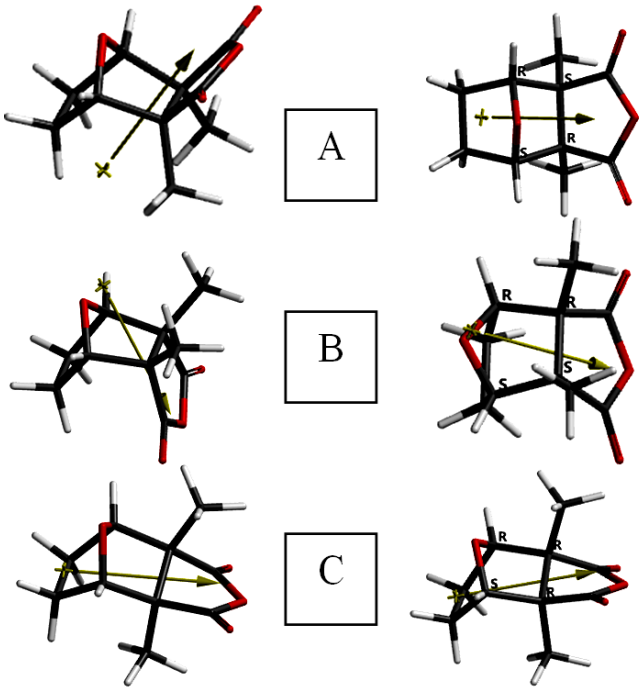

Figure 1. Side and top views of the optimized structures of the isomers considered.

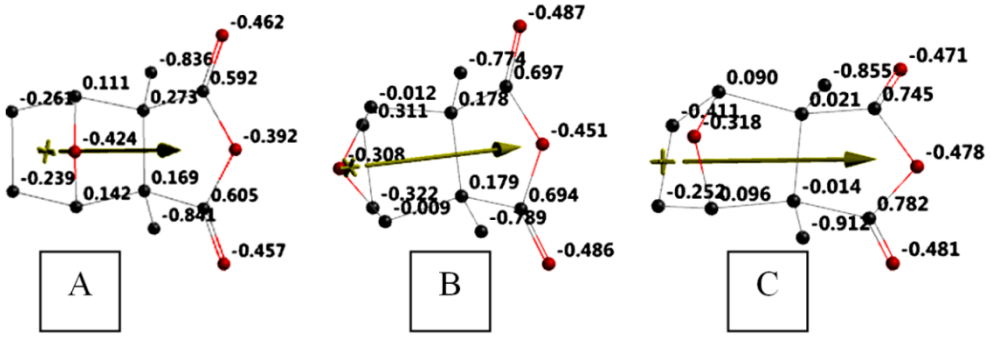

Figure 2. The ESP charges on atoms of the isomers (Hydrogens not shown).

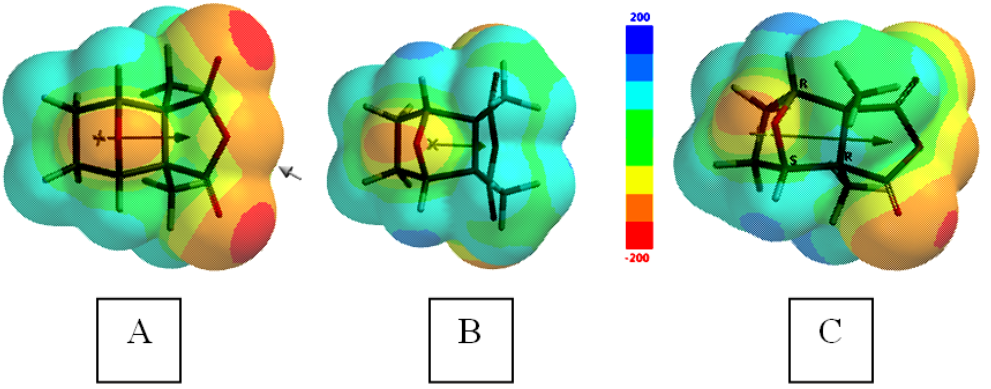

Figure 3. The ESP maps of the isomers considered.

Table 1. Some properties of the isomers considered.

	A	**B**	**C**
Eaq (kJ/mol)	-1810024.42	-1810008.07	-1809803.32
Solvation E (kJ/mol)	-32.41	-21.97	-23.61
Dipole moment (debye)	6.41	3.54	4.70
Polarizability	54.83	54.81	54.72
Log P	0.98	0.98	0.98
Ovality	1.25	1.24	1.22
Conformers	4	4	32

According to the data presented in Table 2, all the isomers possess exothermic standard heat of formation (H^o) and favorable G^o values having the same algebraic orders of A<B<C, whereas the S^o values follow the order of A>B>C, apparently following the order of ovality values (see Tables 1 and 2).

Table 2. Some thermo chemical properties of the isomers considered.

	H^o	S^o (J/mol^o)	G^o
A	-1809425.486	417.06	-1809549.836
B	-1809420.101	416.82	-1809544.378
C	-1809214.084	411.99	-1809336.922

Energies in kJ/mol.

Table 3 lists some energies of the isomers considered where E, ZPE and E_C stand for the total electronic energy, zero point vibrational energy and the corrected total electronic energy, respectively. The data in Table 3 reveal that all the isomer are electronically stable, following the stability order of A>B>C. As the stability order reveals, probably some repulsive interactions between lone pairs of the etheric oxygen and oxygen atoms of the anhydride moiety make B-type isomers less stable than A-type isomers.

Table 3. Some energies of the isomers considered.

Isomer	E	ZPE	E_C
A	-1809992.01	552.72	-1809439.29
B	-1809986.10	552.06	-1809434.04
C	-1809779.70	552.27	-1809227.43

Energies in kJ/mol.

Figure 4 displays some of the molecular orbital energy levels of the isomers considered, whereas the HOMO, LUMO energies (ε_{HOMO} and ε_{LUMO}, respectively) and intermolecular orbital energy gap $\Delta\varepsilon$ ($\Delta\varepsilon = \varepsilon_{LUMO} - \varepsilon_{HOMO}$) values of the tautomers are shown in Table 4. As seen in Figure 4 isomerization also affects the inner-lying molecular orbitals, as well as the NEXTLUMOs.

The HOMO and LUMO energies follow the same order of B<C<A. Whereas, the order of $\Delta\varepsilon$ values is A>B>C which indicates that as going from isomer-A to C a bathochromic effect should arise in the UV-VIS spectra of the isomers considered. Figure 5 displays the calculated UV-VIS spectra of the isomers considered. As seen in the figure, spectrums of the isomers are not very

different from each other in contrast to expectation based on their Δε values. That is because of the fact that the calculated spectra are not only based on the HOMO and LUMO orbital energies but also some other molecular orbital energies are involved. Note that these order of Δε values are dictated by the *endo/exo* orientation of the anhydride moiety and the methyl groups which altogether direct the σ-effects on molecular orbital energies, charge distributions and some long-range interactions occurring through space.

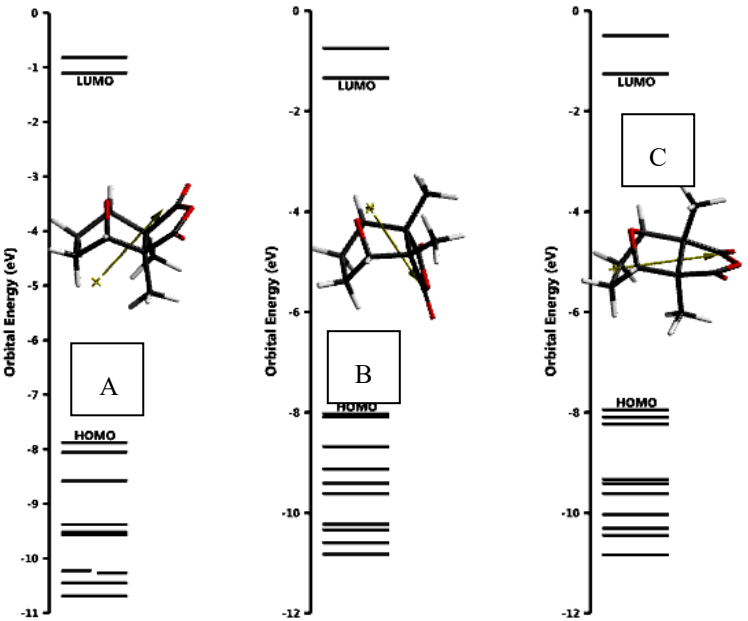

Figure 4. Some of the molecular orbital energy levels of the isomers considered.

Table 4. The HOMO and LUMO energies and Δε values of the isomers considered.

Isomer	HOMO	LUMO	Δε
A	-760.68	-106.81	653.87
B	-774.98	-129.11	645.87
C	-767.25	-121.62	645.63

Energies in kJ/mol.

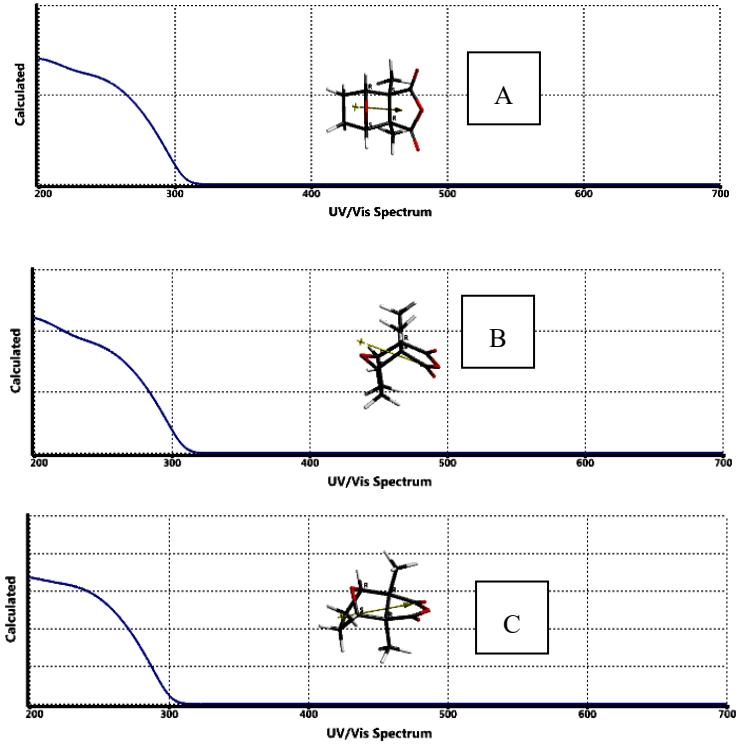

Figure 5. The calculated UV-VIS spectra of the isomers considered.

Figure 6 is the local ionization potential map of the isomers, where conventionally red/reddish regions (if any exists) on the density surface indicate areas from which electron removal is relatively easy, meaning that they are subject to electrophilic attack.

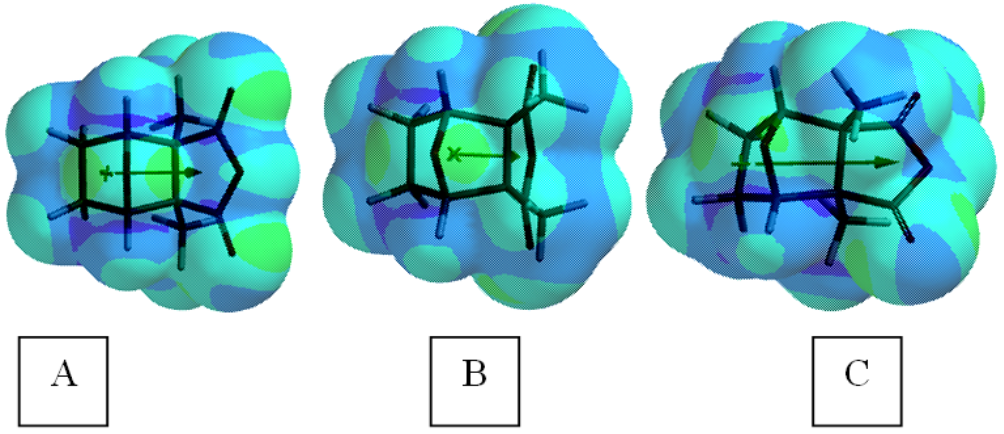

Figure 6. The local ionization potential maps of the isomers considered.

Figure 7 shows the LUMO maps of the isomers considered. Note that a LUMO map displays the absolute value of the LUMO on the electron density surface. The blue color (if any exists) stands for the maximum value of the LUMO and the red-colored region, associates with the minimum value.

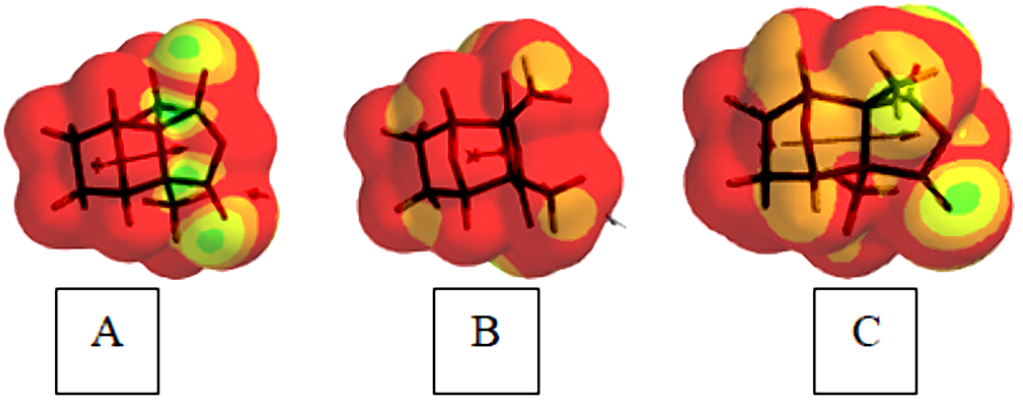

Figure 7. The LUMO maps of the isomers considered.

The Radicals considered

The atmospheric oxidation of C-H bond to a C-O-OH group which is called auto oxidation (hydroperoxidation) is catalyzed by light. As with other free-radical reactions of C-H bonds, some bonds are attacked more readily than others. The reaction may be carried out successfully at tertiary allylic and benzylic positions. The α-position of ethers are also easily attacked by oxygen [28]. Cantharidine possesses such kind of etheric positions. Of course the overall auto oxidation depends on various factors involved in the process, such as bond dissociation energy of C-H bond. The stability of the resultant free-radical formed is also important. In the literature there exist numerous articles about hydro peroxide formation [29-34].

Below (Figure 8), the radicals formed at the α-position of cantharidine are subjected to DFT treatment at the level of UB3LYP/6-31+G(d). They all have C1 symmetry and are labeled as rA1, rA2 … etc., indicating their radical nature and origin as well as the position of the radical formed (see Figure 8).

Figure 9 shows the ESP charges on atoms of the radicals considered. As seen in the figure, depending on the position of the radical formed, the charges are quite different for atoms of the same atom, originated from the same isomer. Namely the charges on rA1 differ from rA2 and rB1 differ from rB2, etc.

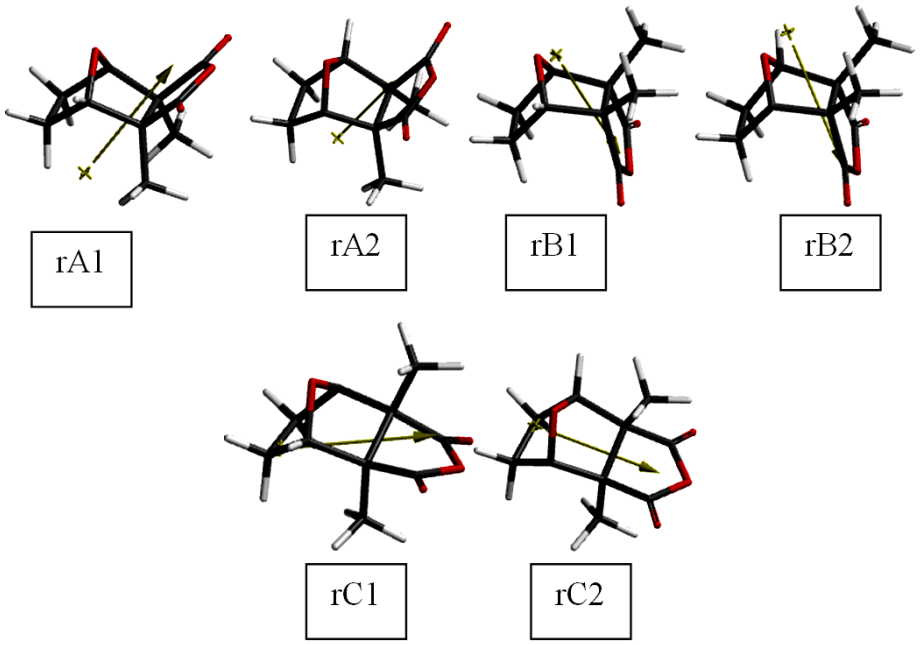

Figure 8. Optimized structures of the radicals from the isomers considered.

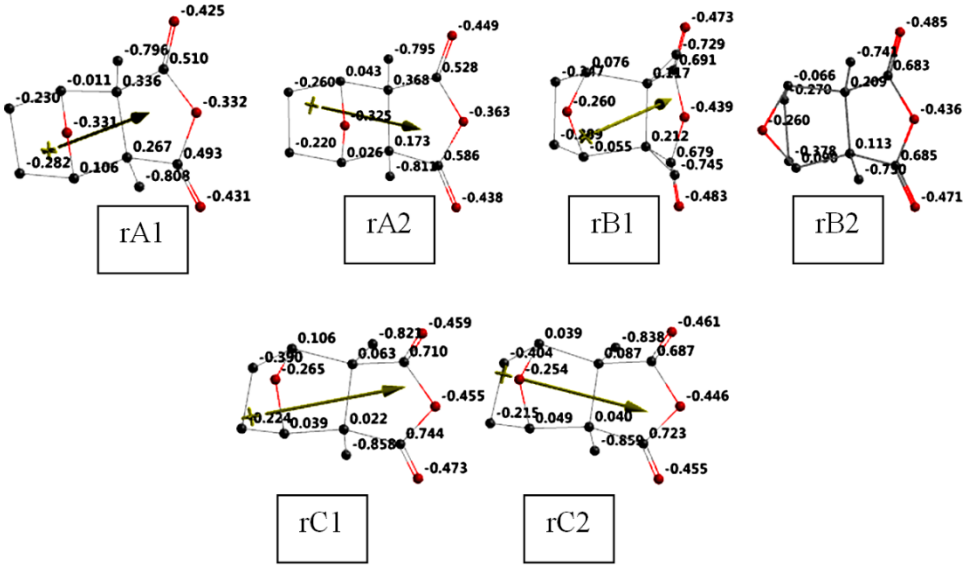

Figure 9. The ESP charges on atoms of the radicals considered (Hydrogens not shown).

Table 5 shows the dipole moment values of the radicals considered. As seen in the table, they are the same for the radicals of the same origin (with the exceptions of rC1 and rC2). The apparent

outcome might be due to the character of the basis set employed or it might be the reality. However, whatever the cause has been the results are such that radicals from isomer-A and isomer-B have the highest and the lowest dipole moment values, respectively.

Table 5. Dipole moment values of the radicals considered.

	rA1	rA2	rB1	rB2	rC1	rC2
Dipole moment	6.73	6.73	3.27	3.27	4.64	4.66

In debye unit

As seen in Table 6, the radicals all have exothermic H^o values and are characterized with favorable G^o values. The order of G^o values is rA2< rA1< rB1< rB2< rC1< rC2.

Table 6. Some thermo chemical properties of radicals from the isomers considered.

Radical	**H^o**	**S^o (J/mol^o)**	**G^o**
rA1	-1807224.734	416.62	-1807348.950
rA2	-1807224.697	416.92	-1807349.002
rB1	-1807221.919	417.49	-1807346.395
rB2	-1807221.830	417.38	-1807346.272
rC1	-1807018.743	411.83	-1807141.531
rC2	-1807013.069	411.22	-1807135.676

Energies in kJ/mol.

Table 7 shows some energies of radicals from the isomers considered. The corrected total electronic energy values (E_C) follow the same order of G^o values (Table 6). Since, these radicals (in terms of the classical theory) are mainly stabilized by resonance effect of the etheric oxygen atom, the calculated stability order mainly reflects the assistance of the oxygen atom. The stabilities follow the order of rA2> rA1> rB1> rB2> rC1> rC2.

Table 7. Some energies of radicals from the isomers considered.

Radical	**E**	**ZPE**	**E_C**
rA1	-1807759.68	521.17	-1807238.51
rA2	-1807759.38	520.84	-1807238.54
rB1	-1807756.12	520.20	-1807235.92
rB2	-1807756.02	520.18	-1807235.84
rC1	-1807552.61	520.50	-1807032.11
rC2	-1807547.47	521.11	-1807026.36

Energies in kJ/mol.

Table 8 lists the HOMO and LUMO energies and Δε values of the radicals considered.

Table 8. The HOMO and LUMO energies and Δε values of the radicals considered.

Radical	HOMO	LUMO	Δε
rA1	-657.35	-117.36	539.99
rA2	-657.92	-117.50	540.42
rB1	-663.98	-140.69	523.29
rB2	-664.47	-140.73	523.74
rC1	-652.00	-129.79	522.21
rC2	-660.93	-129.71	531.22

Energies in kJ/mol.

The HOMO energy order is rB2< rB1< rC2< rA2< rA1< rC1, whereas the LUMO energies follow the order of rB2< rB1< rC1< rC2< rA2< rA1. Consequently, the Δε order is rC1< rB1< rB2< rC2< rA1< rA2. The orders reveal that the stereochemistry of the anhydride moiety is highly influential on the HOMO energies so that the radicals from B-type isomers possess lower energy than the radicals from A-type. The same behavior also holds for the LUMO energies.

Figure 10 displaces the spin densities of the radicals considered. Note that spin density stands for the difference in the number of electrons per unit volume of "up" spin and "down" spin at a point in space. The function is defined over all the space and summed over all space to give the difference in the total number of electrons of "up" and "down" spin [35].

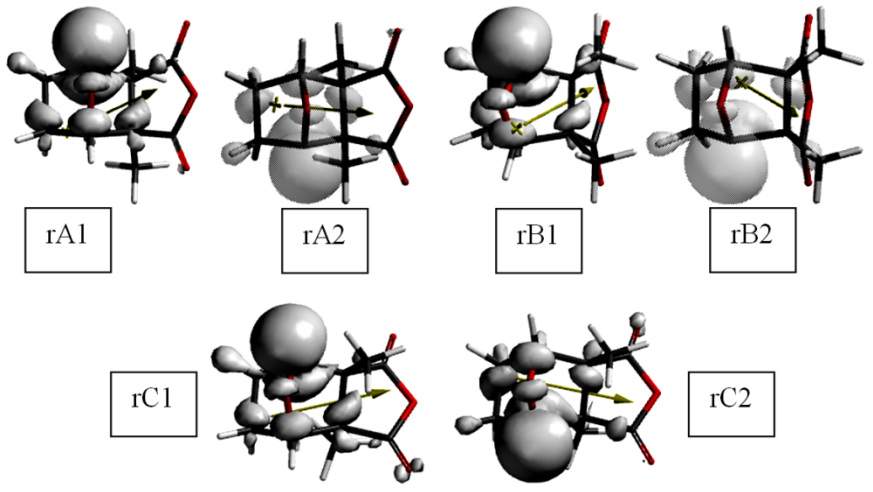

Figure 10. Spin densities of the radicals considered.

As seen in the picture, the spin density accumulates not only on the primary site of radical formation, but distributed over some other sites as well. Those sites up to a certain extent are vulnerable to radical attacks. Figure 11 stands for the spin density maps of the radicals from the isomers considered.

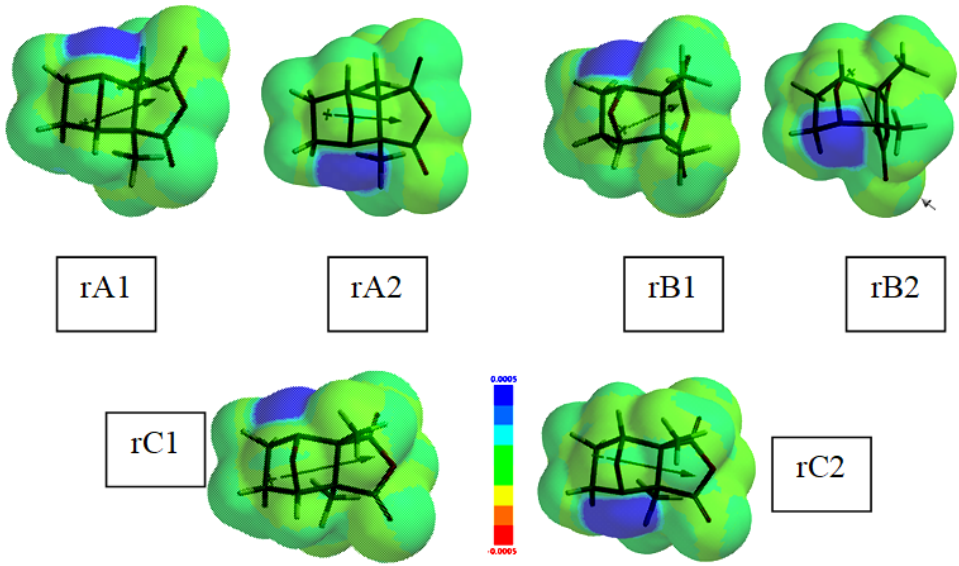

Figure 11. Spin density maps of the radicals from the isomers considered.

Note that a spin density map is a graph that shows the value of the spin density on an electron density isosurface corresponding to a van der Waals surface. By convention, colors blue/bluish indicate high concentration of spin density while colors red/reddish indicate low concentration [35].

4. Conclusion

The present DFT treatment has indicated (within the limitations of the theory and basis set) that in vacuum and aqueous conditions, the isomers considered are electronically stable and have thermo chemically favorable formation values. The stereochemistry highly affects the thermal and electronic properties of the isomers considered. As for the mono radicals formed from the isomers considered by the homolytic cleavage of C-H bond at the α-positions of the etheric oxygen atom, they also have thermo chemically favorable formation values and are electronically stable. Since, cantharidine has many medical usage, the isomers considered might have some medical applicability. They may have more potent activity and low cytotoxicity. On the other hand, the considered isomers and the radicals from them might undergo auto oxidation under certain conditions affecting at least their shelf life.

References

[1] Oaks, W.W., Di Tunno, J.F., Magnani, T., Levy, H.A., & Mills, L.C. (1960). Cantharidine poisoning. *Arch. Intern. Med*., *105*, 574-582. https://doi.org/10.1001/archinte.1960.00270160072009

[2] Wang, G.S. (1989). Medical uses of mylabris in ancient China and recent studies. *J. Ethnopharmacol*., *26*, 147-162. https://doi.org/10.1016/0378-8741(89)90062-7

[3] Galvis, C.E.P., Mendez, L.Y.V., & Kouznetsov, V.V. (2013). Cantharidine-based small molecules as potential therapeutic agents. *Chem. Biol. Drug Des*., *82*, 477. https://doi.org/10.1111/cbdd.12180

[4] Gbaguidi, F.A., Kasséhin, U.C., Prevost, J.R.C., Frederick, R., McCurdy, C.R., & Poupaert, J.H. (2015). Insight into the Diels-Alder reaction: A green chemistry revisitation of the synthesis of a cantharidine-like trypanocidal pilot-molecule. *Journal of Chemical and Pharmaceutical Research*, *7*(7), 1109-1113.

[5] Khan, R.A., Rashid, M., & Naveed, M. (2022). Cantharidin: A chemical precursor for the development of novel bioinsecticides. *Bulgarian Chemical Communications*, *54*(1), 19-28. https://doi.org/10.34049/bcc.54.1.5447

[6] Deng, L.P., Dong, J., Cai, H., & Wang, W. (2013). Cantharidin as an antitumor agent: A retrospective review. *Current Medicinal Chemistry, 20,* 159-166.

[7] Peng, F., Wei, Y.Q., Tian, L., Yang, L., Zhao, X., Lu, Y., Mao, Y.Q., Kan, B., Lei, S., Wang, G.S., Jiang, Y., Wang, Q.R., Luo, F., Zou, L.Q., & Liu, J.Y.J. (2002). Induction of apoptosis by norcantharidin in human colorectal carcinoma cell lines: involvement of the CD95 receptor/ligand. *Cancer Res. Clin. Oncol.*, *128*, 223-230. https://doi.org/10.1007/s00432-002-0326-5

[8] Chen, Y.J., Kuo, C.D., Tsai, Y.M., Yu, C.C., Wang, G.S., & Liao, H.F. (2008). Norcantharidin induces anoikis through Jun-N-terminal kinase activation in CT26 colorectal cancer cells. *Anti-Cancer Drugs*, *19*, 55-64. https://doi.org/10.1097/CAD.0b013e3282f18826

[9] Chen, Y.N., Chen, J.C., Yin, S.C., Wang, G.S., Tsauer, W., Hsu, H.F., & Hsu, S.L. (2002). Effector mechanisms of norcantharidin-induced mitotic arrest and apoptosis in human hepatoma cells. *Int. J. Cancer*, *100*, 158-165. https://doi.org/10.1002/ijc.10479

[10] Williams, L.A., Moller, W., Merisor, E., Kraus, W., & Rosner, H. (2003). *In vitro* antiproliferation/cytotoxic activity of cantharidin (Spanish fly) and related derivatives. *West. Ind. Med. J*., *52*, 10-13. PMID: 12806747.

[11] Huh, J.E., Kang, K.S., Chae, C., Kim, H.M., Ahn, K.S., & Kim, S.H. (2004). Roles of

p38 and JNK mitogen-activated protein kinase pathways during cantharidin-induced apoptosis in U937 cells. *Biochem. Pharmacol*., *67*, 1811-1818. https://doi.org/10.1016/j.bcp.2003.12.025

[12] Wu, J.Z., Situ, Z.Q., Chen, J.Y., Liu, B., & Wang, W. (1992). Chemosensitivity of salivary gland and oral cancer cell lines. *Chin. Med. J*., *105*, 1026-1028.

[13] Kok, S.H., Chui, C.H., Lam, W.S., Chen, J., Tang, J.C., Lau, F.Y., Cheng, G.Y., Wong, R.S., & Chan, A.S. (2006). Apoptotic activity of a novel synthetic cantharidin analog on hepatoma cell lines. *Int. J. Mol. Med*., *17*, 945-949. https://doi.org/10.3892/ijmm.17.5.945

[14] Kok, S.H., Chui, C.H., Lam, W.S., Chen, J., Tang, J.C., Lau, F.Y., Cheng, G.Y., Wong, R.S., & Chan, A.S. (2006). Apoptogenic activity of a synthetic cantharimide in leukaemia: implication on its structural activity relationship. *Int. J. Mol. Med*., *18*, 1217-1221. https://doi.org/10.3892/ijmm.18.6.1217

[15] Li, W., Xie, L., Chen, Z., Zhu, Y., Sun, Y., Miao, Y., Xu, Z., & Han, X. (2010). Cantharidin, a potent and selective PP2A inhibitor, induces an oxidative stress independent growth inhibition of pancreatic cancer cells through G2/M cellcycle arrest and apoptosis. *Cancer Sci*., *101*, 1226-1233. https://doi.org/10.1111/j.1349-7006.2010.01523.x

[16] Recanati, M.A., Kramer, K.J., Maggio, J.J., & Chao, C.R. (2018). Cantharidin is superior to trichloroacetic acid for the treatment of non-mucosal genital warts: A pilot randomized controlled trial, *Clin. Exp. Obstet. Gynecol*., *45*(3), 383-386. https://doi.org/10.12891/ceog4112.2018

[17] Coloe, J., & Morrell, D.S. (2009). Cantharidin use among pediatric dermatologists in the treatment of *Molluscum Contagiosum*, *Pediatric Dermatology*, *26*(4), 405-408. https://doi.org/10.1111/j.1525-1470.2008.00860.x

[18] Torbeck, R., Pan, M., de Moll, E., & Levitt, J. (2014). Cantharidin: a comprehensive review of the clinical literature, *Dermatology Online Journal*, *20*(6). https://doi.org/10.5070/d3206022861

[19] Stewart, J.J.P. (1989). Optimization of parameters for semi empirical methods I. *J. Comput. Chem*., *10*, 209-220. https://doi.org/10.1002/jcc.540100208

[20] Stewart, J.J.P. (1989). Optimization of parameters for semi empirical methods II. *J. Comput. Chem*., *10*, 221-264. https://doi.org/10.1002/jcc.540100209

[21] Leach, A.R. (1997). *Molecular modeling*. Essex: Longman.

[22] Kohn, W., & Sham, L.J. (1965). Self-consistent equations including exchange and

correlation effects. *Phys. Rev*., *140*, 1133-1138. https://doi.org/10.1103/PhysRev.140.A1133

[23] Parr, R.G., & Yang, W. (1989). *Density functional theory of atoms and molecules*. London: Oxford University Press.

[24] Becke, A.D. (1988). Density-functional exchange-energy approximation with correct asymptotic behavior. *Phys. Rev. A*, *38*, 3098-3100. https://doi.org/10.1103/PhysRevA.38.3098

[25] Vosko, S.H., Wilk, L., & Nusair, M. (1980). Accurate spin-dependent electron liquid correlation energies for local spin density calculations: a critical analysis. *Can. J. Phys.*, *58*, 1200-1211. https://doi.org/10.1139/p80-159

[26] Lee, C., Yang, W., & Parr, R.G. (1988). Development of the Colle-Salvetti correlation energy formula into a functional of the electron density. *Phys. Rev. B*, *37*, 785-789. https://doi.org/10.1103/PhysRevB. 37.785

[27] SPARTAN 06 (2006). Wavefunction Inc. Irvine CA, USA.

[28] March, J. (1968). *Advanced organic chemistry*. Tokyo: McGraw-Hill Kogakusha.

[29] Watkins, J.M., Mushrush, G.W., Hazlett, R.N., & Beal, E.J. (1989). Hydroperoxide formation and reactivity in jet fuels. *Energy Fuels*, *3*, 231-6. https://doi.org/10.1021/ef00014a018

[30] Mushrush, G.W., Beal, E.J., Hughes, J.M., Bonde, S.E., Gore, W.L., & Dolbear, G.E. (2002). Stability studies of a jet fuel containing no organo-sulfur compounds. *Pet. Sci. Technol*., *20*(5-6), 561-70. https://doi.org/10.1081/LFT-120003580

[31] Fodor, G.E., Naegeli, D.W., & Kohl, K.B. (1988). Peroxide formation in jet fuels. *Energy Fuels*, *2*(6), 729-34. https://doi.org/10.1021/ef00012a002

[32] Black, B.H., Hardy, D.R., & Beal, E.J. (1991). Accelerated hydroperoxide formation in jet fuel at 65 C in capped and vented bottles. *Energy Fuels*, *5*(2), 281-2. https://doi.org/10.1021/ef00026a010

[33] Zabarnick, S., & Phelps, D.K. (2006). Density functional theory calculations of the energetics and kinetics of jet fuel autoxidation reactions. *Energy Fuels*, *20*(2), 488-97. https://doi.org/10.1021/ef050348l

[34] Türker, L., Varis, S., & Bayar, Ç,Ç. (2013). A theoretical study of JP-10 hydroperoxidation. *Fuel*, *104*, 128-132. https://doi.org/10.1016/j.fuel.2012.09.024

[35] Hehre, W.J, Shusterman, A.J., & Huang, W.W. (1998). *A laboratory book of computational organic chemistry*. Irving, CA: Wavefunction.